Supporting Information

Phosphorescent platinum(II) complexes based on spiro linkage-containing ligands

Guojun Liu,[†a] Feng Liang,[†a] Yue Zhao,[b] Hailiang Hu,[a] Jian Fan,*[a] and Liang-Sheng Liao[a]

[a] Jiangsu Key Laboratory for Carbon-Based Functional Materials & Devices, Institute of Functional Nano & Soft Materials (FUNSOM), Soochow University, Suzhou, Jiangsu 215123, China

[b] Coordination Chemistry Institute, State Key Laboratory of Coordination Chemistry, School of Chemistry and Chemical Engineering, Nanjing National Laboratory of Microstructures, Collaborative Innovation Center of Advanced Microstructures, Nanjing University, Nanjing 210023, China.

*E-mail: jianfan@suda.edu.cn

[†] Equal Contributors

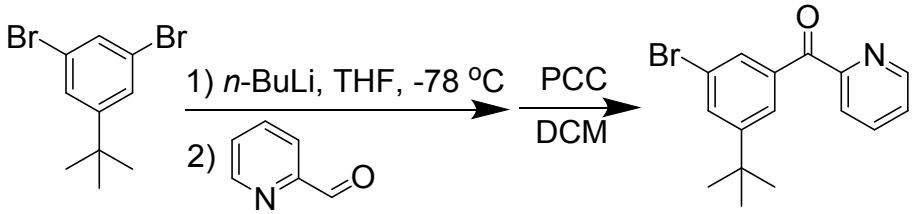

a

To a solution of 1,3-dibromo-5-*tert*-butyl-benzene (12 g, 41.5 mmol) in THF (100 mL) at -78 ºC under N_2, *n*-BuLi (1.6 M, 27 mL) was added dropwise. The reaction mixture was stirred for 2 hours and then pyridine-2-carbaldehyde (4.42 g, 41.5 mmol) was added slowly. Then the reaction system was stirred at room temperature overnight before quenched with water. After the removal of solvent, the residue was extracted with DCM (3×100 mL) and washed with water. The combined organic phase was dried over $MgSO_4$. After the removal of precipitate by filtration, PCC (26.8 g, 124.5 mmol) and 20 g of celite were added to the filtrate. The mixture was stirred at room temperature for 12 hours. The celite was removed by filtration and washed with DCM. The product was purified by column chromatography (SiO_2, DCM:PE, 1:5) to afford a white solid (7.8 g, 59.5%). ^{1}H NMR (400 MHz, *d6*-DMSO) δ 8.73 (d, *J* = 4.1 Hz, 1H), 8.14 – 8.00 (m, 2H), 7.95 (d, *J* = 16.4 Hz, 2H), 7.84 (s, 1H), 7.74 – 7.63 (m, 1H), 1.30 (s, 9H). GC-MS: m/z calcd 317.04, found 317.03.

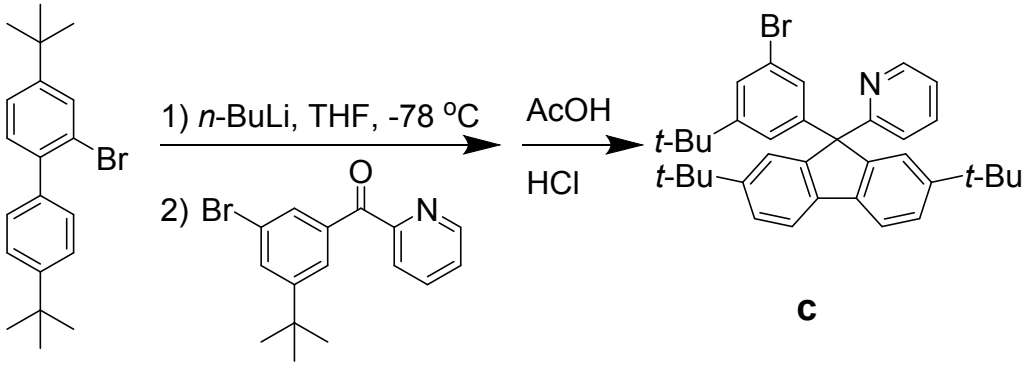

c

To a solution of 2-bromo-4,4'-di-*tert*-butyl-1,1'-biphenyl (5 g, 14.6 mmol) in THF (100 mL) at -78 ºC under N_2, *n*-BuLi (1.6 M, 10 mL) was added dropwise. This mixture was stirred for 2 hours before the addition of compound **a** (4.6 g, 14.6 mmol). Then the reaction system was stirred at room temperature overnight before quenched with water. The solvent was removed under reduce pressure and the residue was extracted with DCM (3×100 mL). The organic phase was combined and washed with water. After the removal of solvent, the residue was then dissolved in the mixture of AcOH (100 mL)

and HCl (3 mL). The mixture was heated at 130 °C for 12 hours before the removal of solvent. The product was purified by column chromatography (SiO_2, DCM:PE, 3:1) to afford a pale yellow solid (6.1 g, 74.4%). ^{1}H NMR (400 MHz, $CDCl_3$) δ 8.66 (d, *J* = 3.9 Hz, 1H), 7.65 (d, *J* = 8.0 Hz, 2H), 7.60 (s, 2H), 7.43 (dd, *J* = 19.3, 7.8 Hz, 3H), 7.32 (s, 1H), 7.11 (d, *J* = 11.2 Hz, 2H), 6.98 (s, 1H), 6.90 (d, *J* = 7.9 Hz, 1H), 1.30 (s, 18H), 1.18 (s, 9H). LC-MS: m/z calcd 565.2, found 565.3.

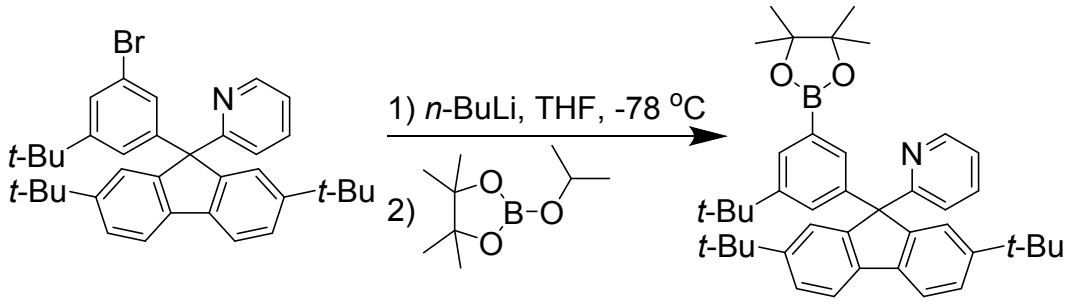

c **d**

To a solution of compound **c** (3 g, 5.3 mmol) in THF (100 mL) at -78 °C under N_2, *n*-BuLi（1.6 M, 3.5 mL）was added dropwise. The reaction mixture was allowed to stir for 2 hours followed by the addition of 2-isopropoxy-4,4,5,5-tetram-ethyl-1,3,2-dioxaborolane (1.0 g, 5.3 mmol). Then the solution was stirred overnight at room temperature. After quenched with water, the reaction system was extracted with DCM. After the removal of the solvent, the residue was used for the next step without any further purification.

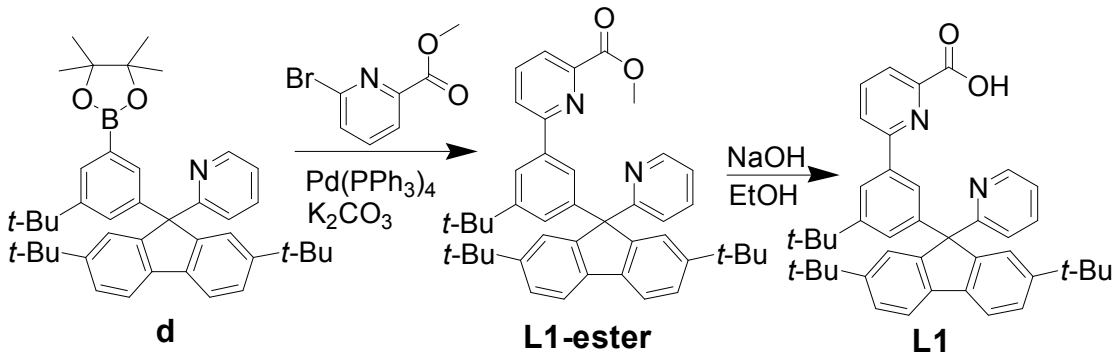

d **L1-ester** **L1**

Synthesis of **L1-ester**: Methyl 6-bromopicolinate (0.89 g, 4.1 mmol), compound **d** (2.5 g, 4.1 mmol), K_2CO_3 (2.8 g, 20.5 mmol) and $Pd(PPh_3)_4$ (0.47 g, 0.41 mmol) were added into a mixture of toluene (25 mL) and water (5 mL) under N_2. The reaction system was heated to reflux overnight. After cooling downing to room temperature, the mixture was extracted with DCM. The ester was purified by column chromatography

(SiO_2, DCM) to afford a pale yellow solid (1.5 g, 61.0%). ^{1}H NMR (400 MHz, *d6*-DMSO) δ 8.56 (s, 1H), 7.96 (dd, *J* = 22.6, 7.6 Hz, 3H), 7.86 (s, 1H), 7.79 (d, *J* = 7.2 Hz, 2H), 7.70 (s, 2H), 7.64 (s, 2H), 7.45 (d, *J* = 7.7 Hz, 2H), 7.22 (s, 2H), 7.01 (d, *J* = 7.3 Hz, 1H), 3.86 (s, 3H), 1.28 (s, 18H), 1.21 (s, 9H). LC-MS: m/z calcd 622.4, found 622.5.

Synthesis of **L1**: The ester (1.4 g, 2.3 mmol), NaOH (3.7 g, 92.1 mmol) and anhydrous ethanol (40 mL) were added into a 125 mL round-bottom flask under N_2. The reaction mixture was heated to reflux overnight. After cooling downing to room temperature, the reaction mixture was acidified to pH = 6 with 2 M HCl. The aqueous phase was extracted by DCM. The target acid compound was obtained by the removal of organic solvent.

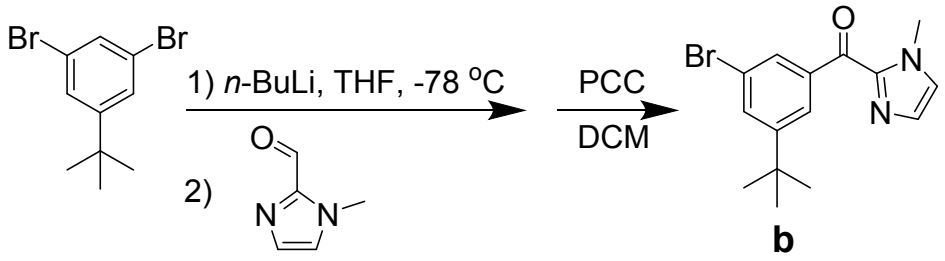

Compound **b** was prepared by the same procedure as that of compound **a** (55.2%). ^{1}H NMR (400 MHz, $CDCl_3$) δ 8.29 (s, 1H), 8.18 (s, 1H), 7.70 (s, 1H), 7.24 (s, 1H), 7.12 (s, 1H), 4.08 (s, 3H), 1.35 (s, 9H). GC-MS: m/z calcd 321.06, found 321.11.

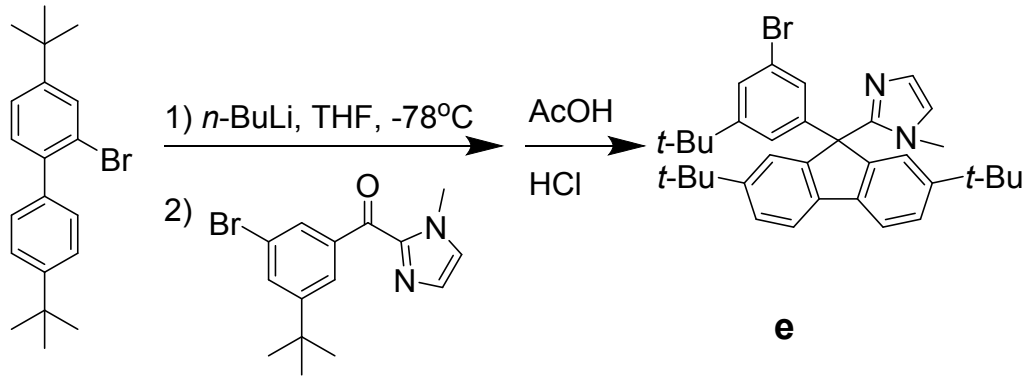

Compound **e** was prepared by the same procedure as that of compound **c** (60.0%)。 ^{1}H NMR (400 MHz, *d6*-DMSO) δ 7.83 (d, *J* = 7.9 Hz, 2H), 7.48 (d, *J* = 8.0 Hz, 2H), 7.35 (s, 3H), 7.29 (s, 1H), 7.16 (s, 1H), 7.00 (s, 1H), 6.83 (s, 1H), 2.58 (s, 3H), 1.25 (s, 18H), 1.15 (s, 9H). LC-MS: m/z calcd 568.2, found 568.4.

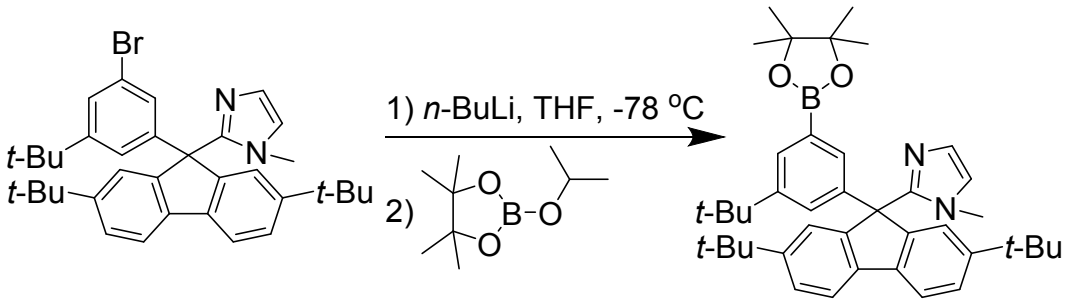

e **f**

Compound **f** was prepared by the same procedure as that of compound **d**. Compound **f** was used for next step without any further purification.

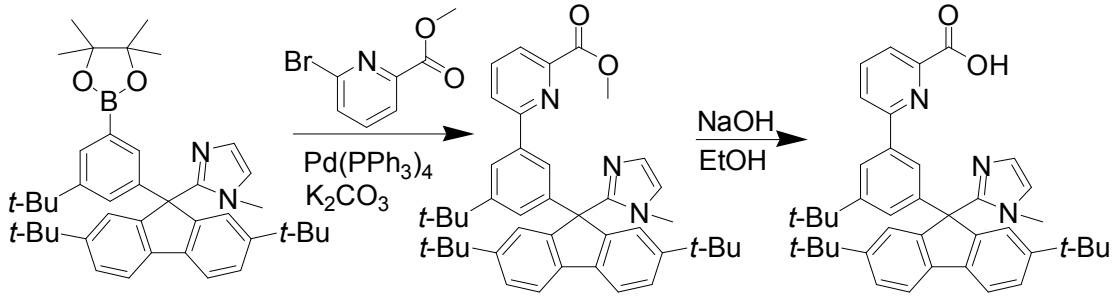

f **L2-ester** **L2**

The synthesis of **L2-ester**: The **L2-ester** was prepared by the same procedure as that of **L1-ester** (74.0%). ^{1}H NMR (400 MHz, *d6*-DMSO) δ 8.02 (d, J = 4.0 Hz, 2H), 7.98 – 7.92 (m, 1H), 7.89 (d, J = 6.2 Hz, 2H), 7.82 (d, J = 7.8 Hz, 2H), 7.48 (d, J = 7.9 Hz, 4H), 7.36 (s, 1H), 7.00 (s, 1H), 6.79 (s, 1H), 3.88 (s, 3H), 2.65 (s, 3H), 1.27 (s, 18H), 1.23 (s, 9H). LC-MS: m/z calcd 625.4, found 625.6.

The synthesis of **L2**: The **L2** was prepared by the same procedure as that of **L1**.

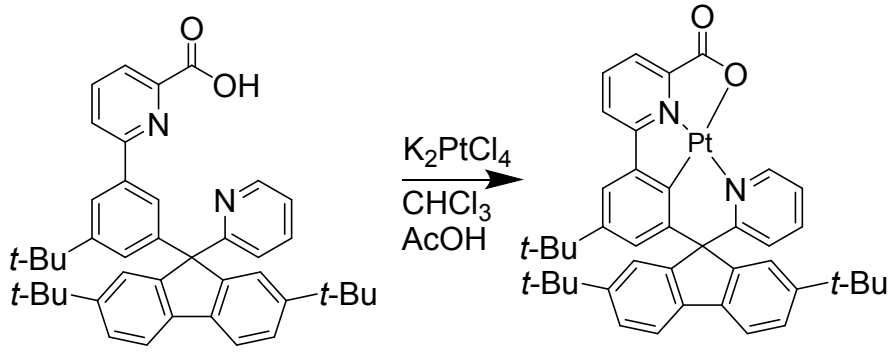

L1 **Pt1**

The synthesis of **Pt1**: Ligand **L1** (1 g, 1.6 mmol) and K_2PtCl_4(0.75 g, 1.8 mmol) were added into a mixture of AcOH (21 mL) and chloroform (3 mL) under N_2. The reaction mixture was allowed to reflux for 4 days. After the removal of solvent, the residue was purified by column chromatography (SiO_2, DCM) to afford a pale yellow solid (0.6 g, 46.0%). ^{1}H NMR (400 MHz, *d6*-DMSO) δ 9.18 (d, *J* = 5.2 Hz, 1H), 8.24 (d, *J* = 8.0 Hz, 1H), 8.16 (t, *J* = 7.8 Hz, 1H), 7.92 (s, 3H), 7.84 (d, *J* = 8.0 Hz, 2H), 7.76 – 7.66 (m, 2H), 7.54 (t, *J* = 6.4 Hz, 1H), 7.47 (d, *J* = 7.9 Hz, 2H), 6.89 (d, *J* = 8.2 Hz, 1H), 6.19 (s, 1H), 1.20 (s, 18H), 0.97 (s, 9H). ^{13}C NMR (600 MHz, $CDCl_3$) δ 172.72, 163.67, 161.39, 152.65, 152.09,152.02, 147.21, 143.76, 139.35, 139.19, 138.34, 137.42, 131.09, 126.62, 125.52,125.42, 123.63, 122.94, 122.82, 120.85, 119.83, 119.67, 71.69, 35.19, 34.51, 31.59, 31.10. HRMS[ESI]: [M+Na] calcd 824.2792, found 824.2778.

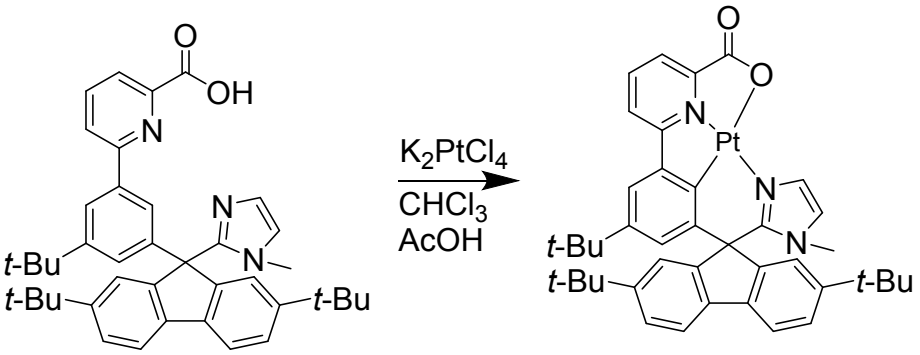

L2 **Pt2**

The synthesis of **Pt2**: The **Pt2** was prepared by the same procedure as that of **Pt1** (54.0%). ^{1}H NMR (400 MHz, *d6*-DMSO) δ 8.15 (dt, *J* = 15.7, 7.9 Hz, 2H), 7.95 (d, *J* = 8.0 Hz, 2H), 7.68 (d, *J* = 7.6 Hz, 1H), 7.60 (s, 1H), 7.54 (d, *J* = 8.0 Hz, 2H), 7.31 (s, 1H), 7.28 (s, 1H), 7.21 (s, 2H), 6.05 (s, 1H), 2.56 (s, 3H), 1.99 (s, 3H), 1.17 (s, 18H), 0.88 (s, 9H). ^{13}C NMR (600 MHz, $CDCl_3$) δ 174.17, 163.36, 152.78, 150.70, 149.69, 146.58, 144.58, 144.20, 139.75, 138.46, 138.24, 128.62, 128.38, 126.95, 125.87, 124.30, 122.77, 121.94, 120.56, 119.68, 63.51, 35.15, 35.11,34.35, 31.53, 30.95. HRMS[ESI]: [M+Na] calcd 826.2880, found 826.2840.

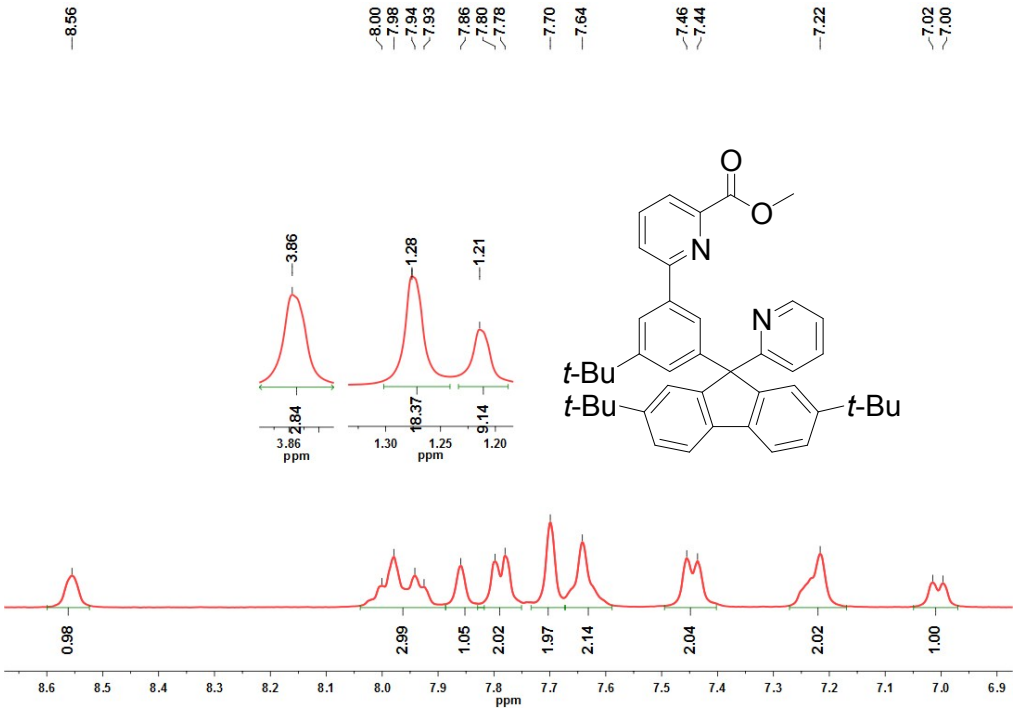

Figure S1. ^{1}H NMR spectrum of ligand of **L1-ester** (*d6*-DMSO)

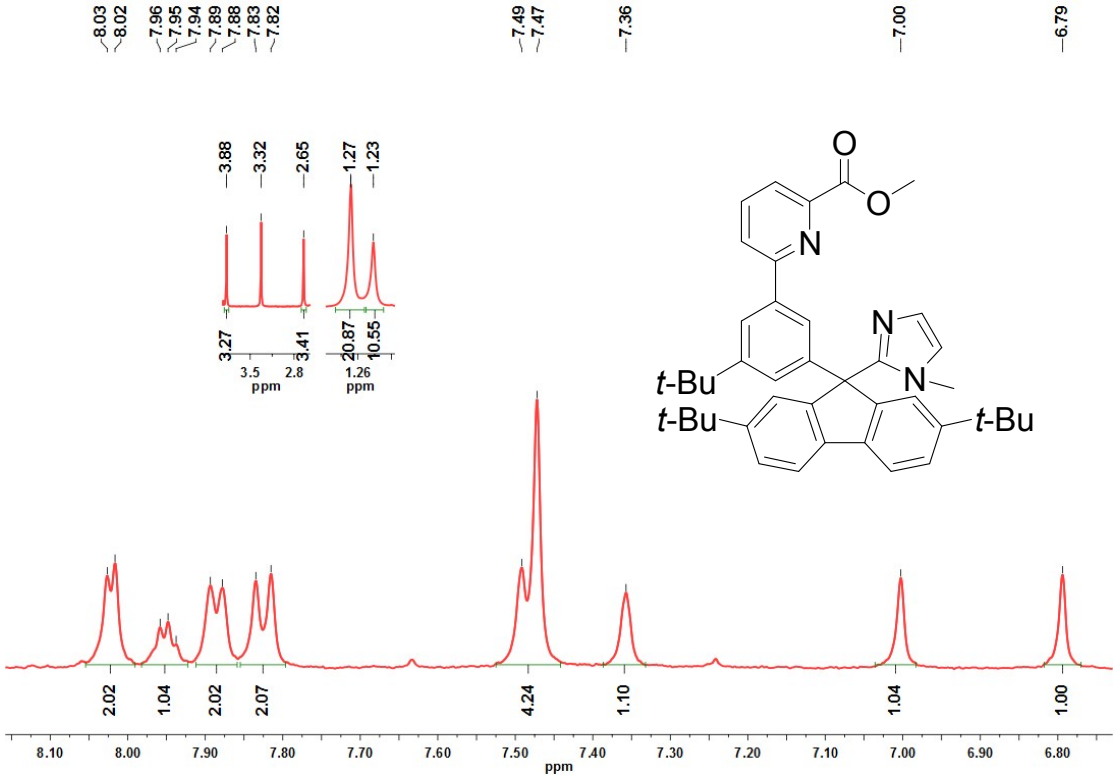

Figure S2. ^{1}H NMR spectrum of ligand of **L2-ester** (*d6*-DMSO)

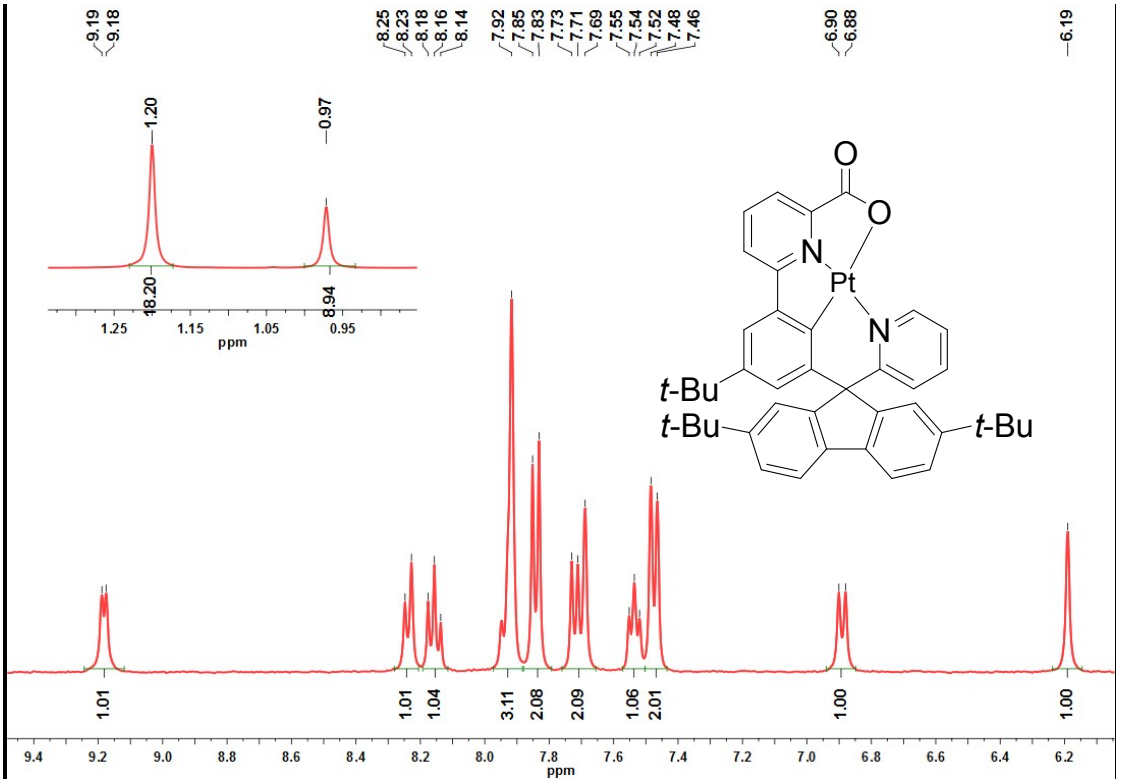

Figure S3. ^{1}H NMR spectrum of complex of **Pt1**(*d6*-DMSO)

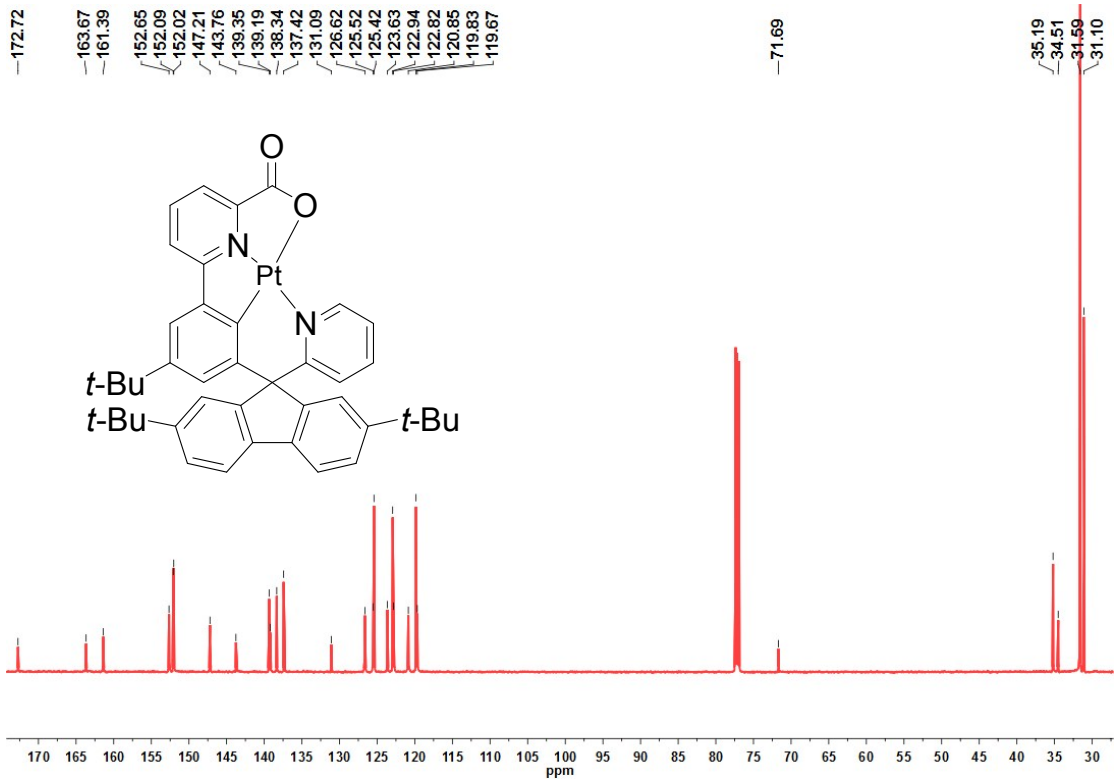

Figure S4. ^{13}C NMR spectrum of complex of **Pt1**($CDCl_3$)

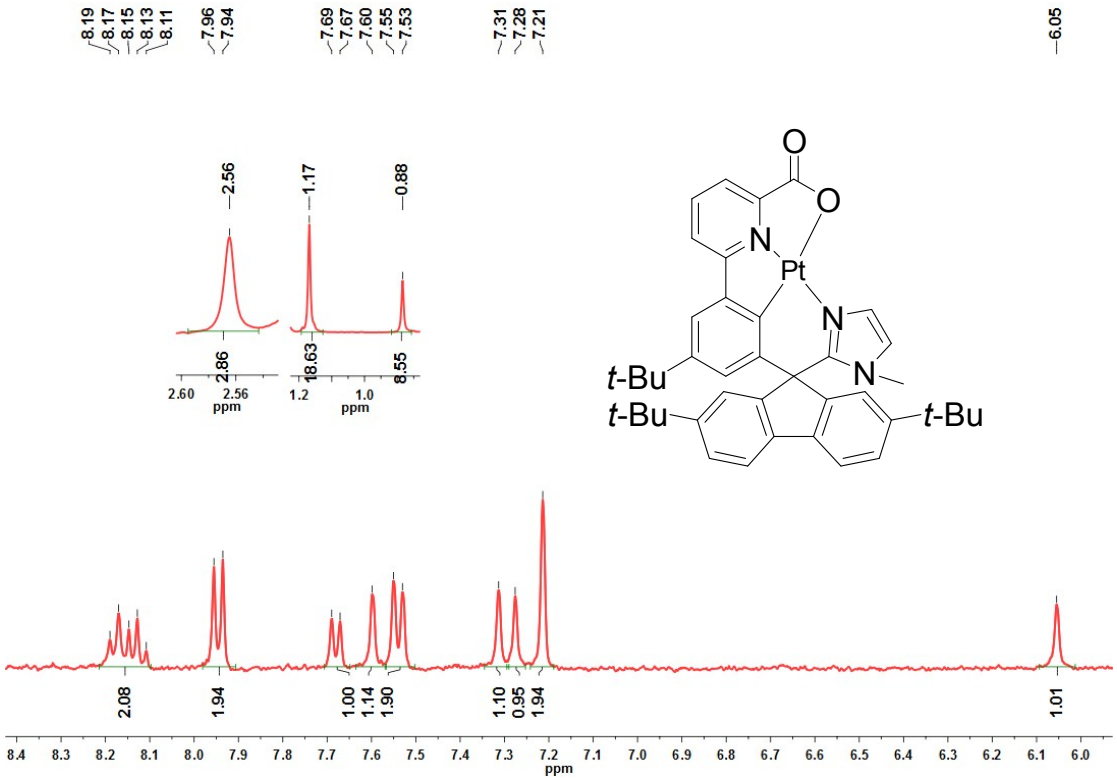

Figure S5. ^{1}H NMR spectrum of complex of **Pt2**(*d6*-DMSO)

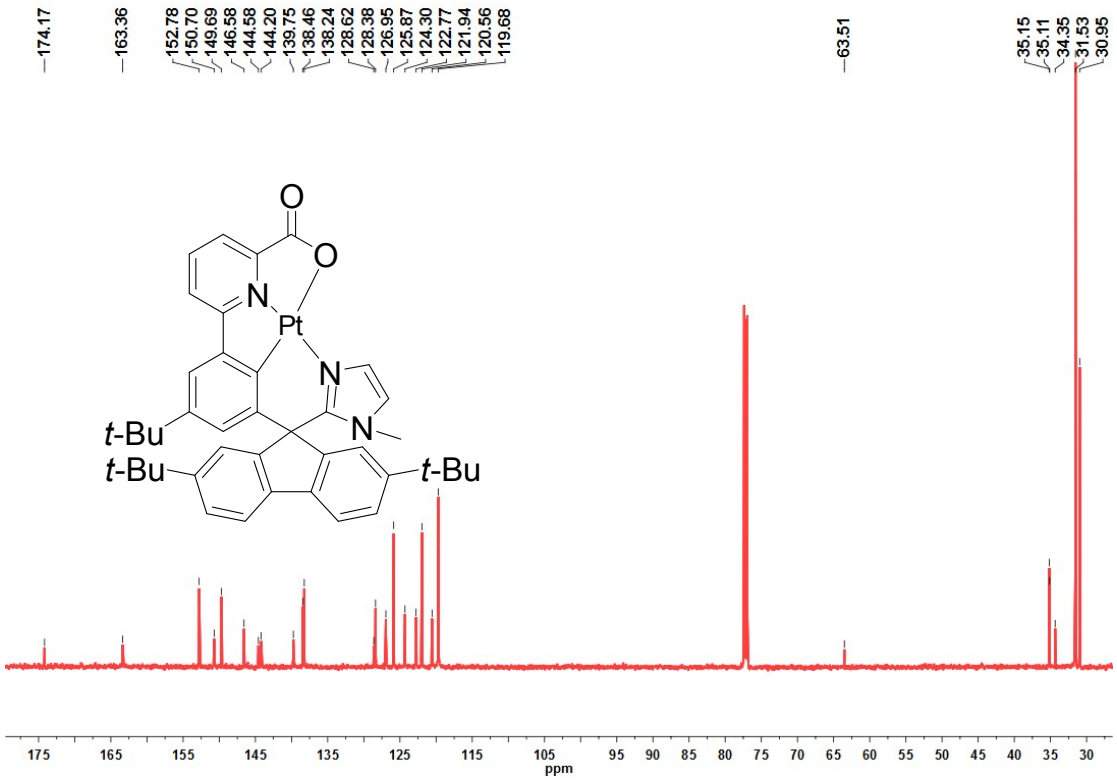

Figure S6. ^{13}C NMR spectrum of complex of **Pt2**($CDCl_3$)

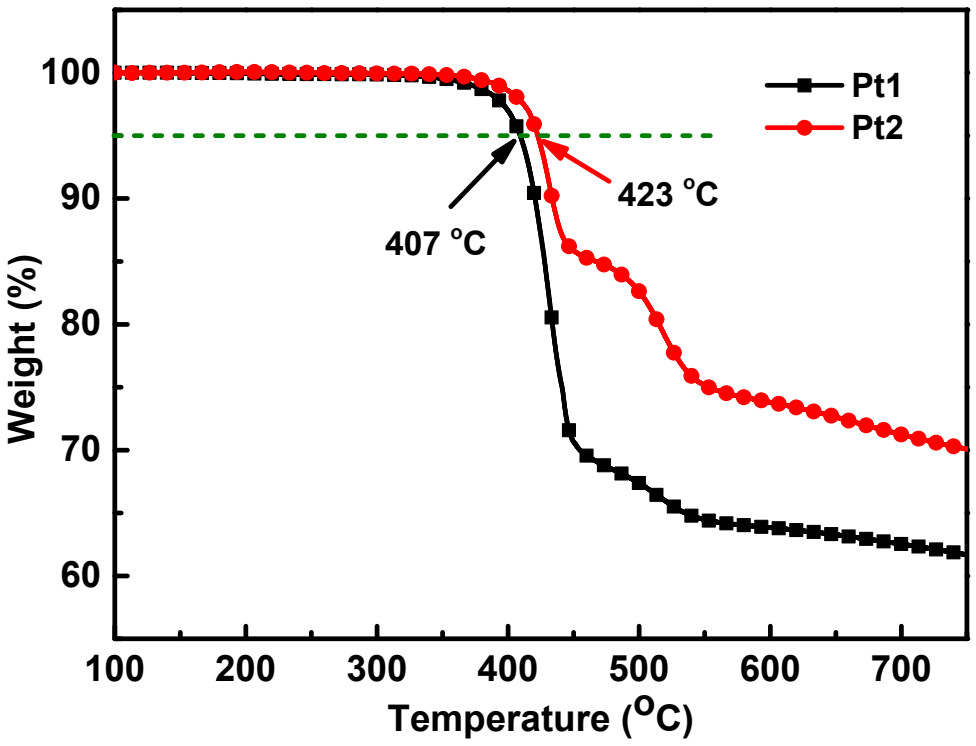

Figure S7. The TGA curves of **Pt1** and **Pt2** at a heating rate of 10 °C /min under N_2.

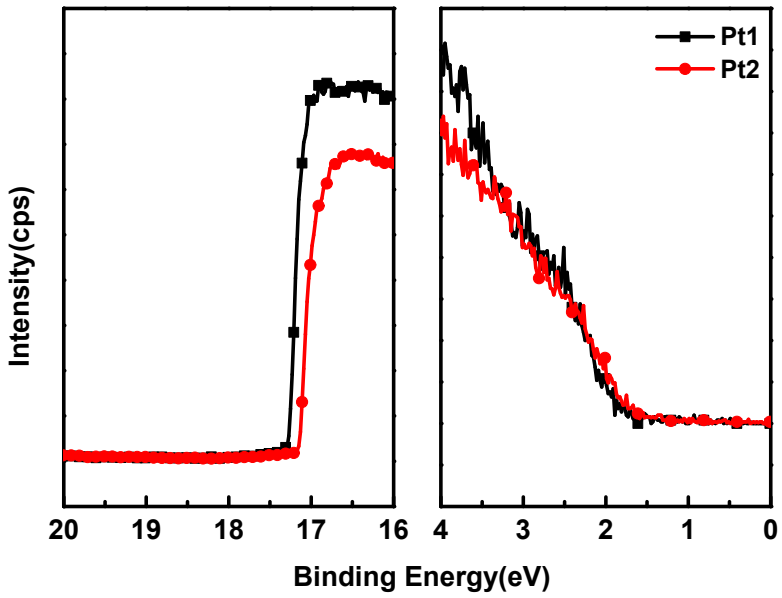

Figure S8. The UPS spectra of **Pt1** and **Pt2**.

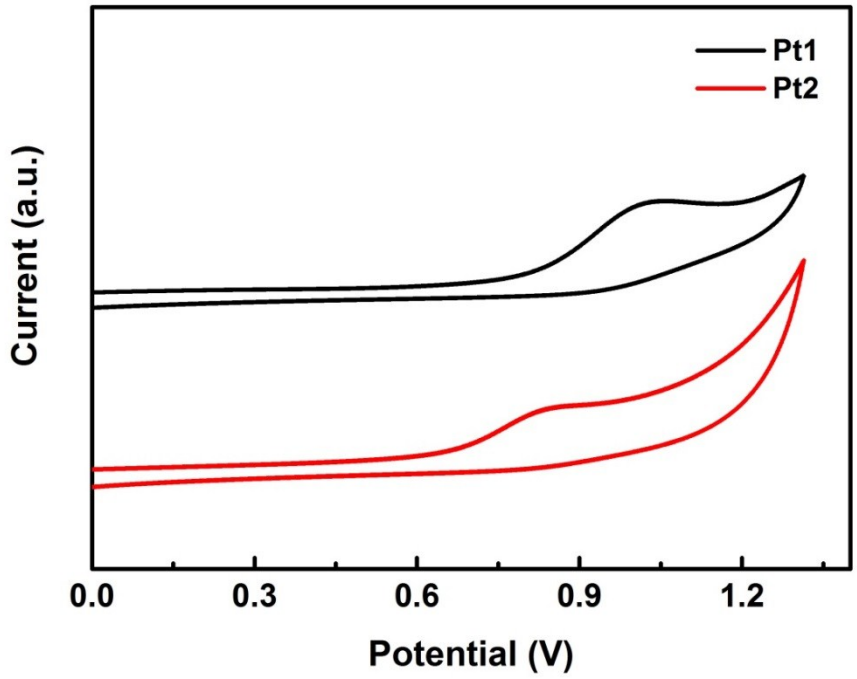

Figure S9. Cyclic voltammograms of **Pt1** and **Pt2** in DMF at 293 K with the Fc^{+}/Fc couple used as the reference.

Table S1. Electrochemical data of **Pt1** and **Pt2**.

	LUMO [eV] [a]	HOMO [eV] [b]	Eg [eV] [c]
Pt1	-2.34	-5.62	3.28
Pt2	-2.31	-5.53	3.22

[a)] LUMO= HOMO + E_g. [b)] Estimated from onset potentials using $FeCp_2^{+/0}$ values of 4.8 eV below the vacuum level. [c)] The optical band gap estimated from the absorption spectra.

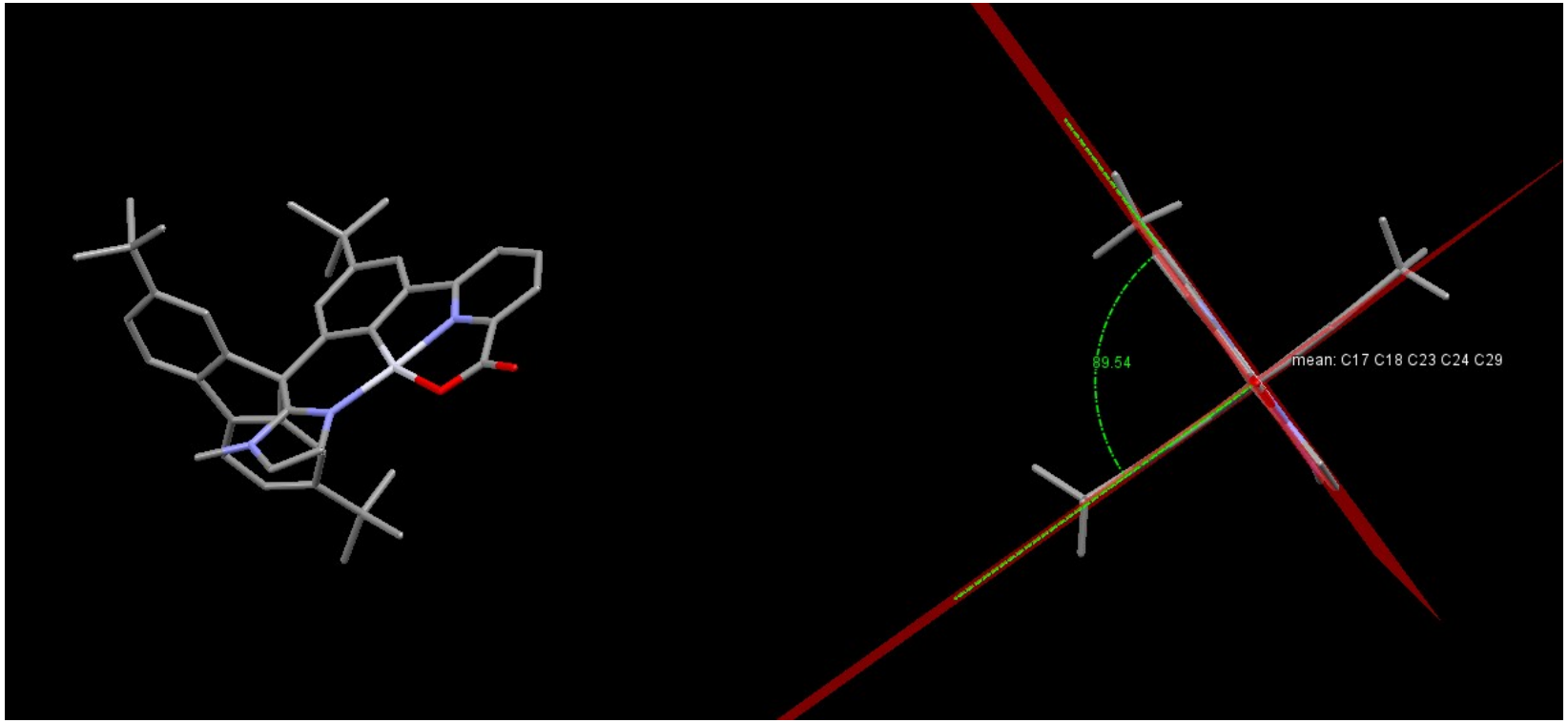

Figure S10. The dihedral angle between the biphenyl group and the rigid coordinating plane in **Pt2**.

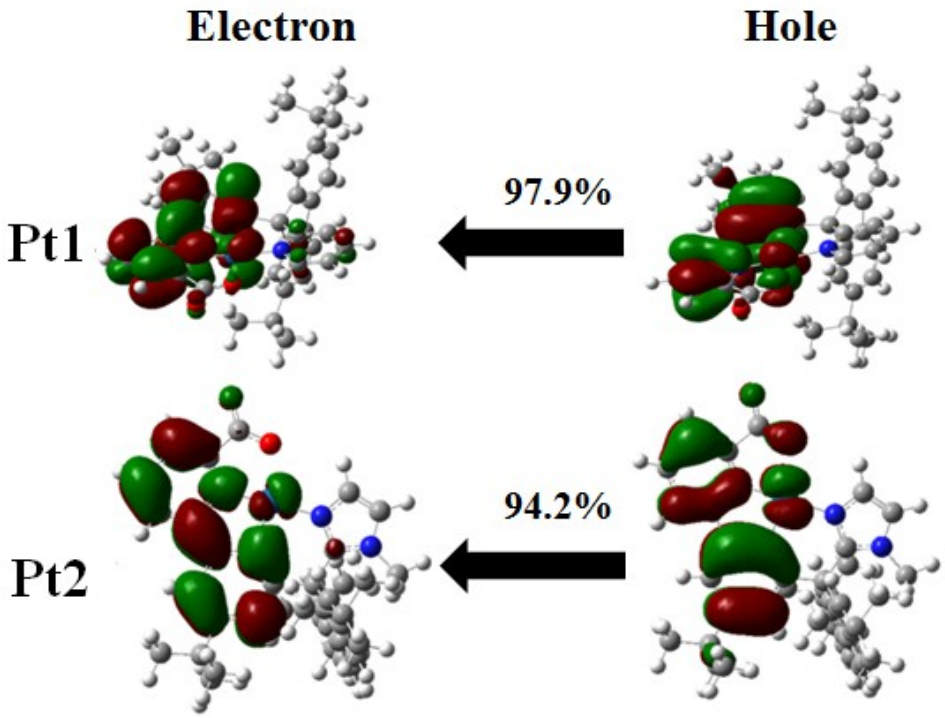

Figure S11. Natural transition orbitals (NTO) analyses for triplet emission of compounds **Pt1** and **Pt2.**

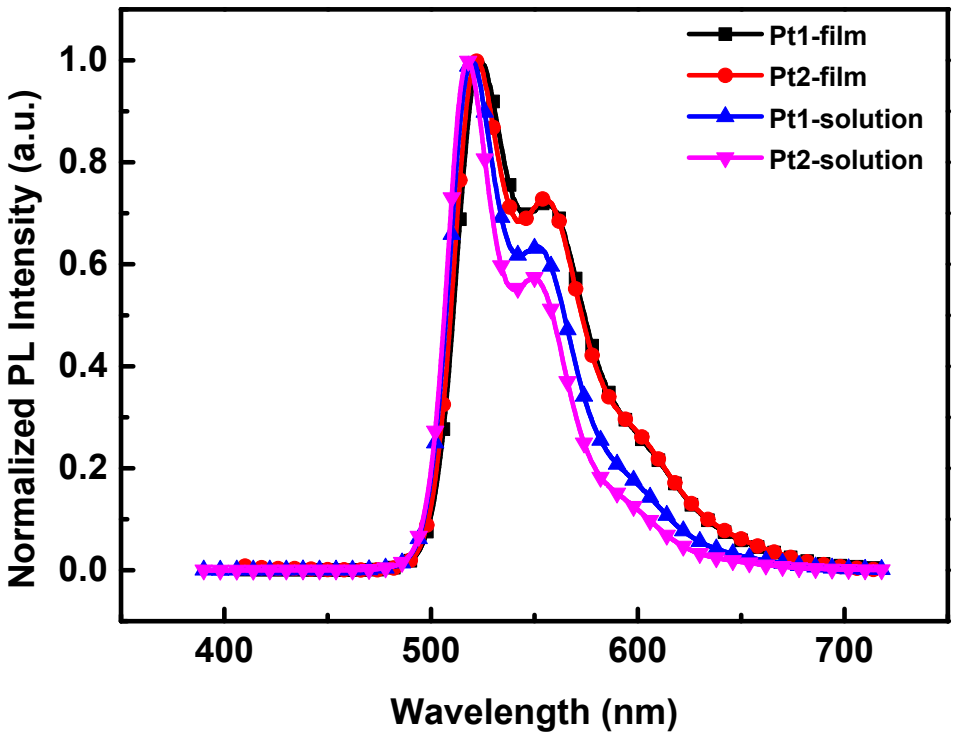

Figure S12. Photoluminescence spectra of **Pt1** and **Pt2** in dilute dichloromethane solution and in neat film at room temperature.

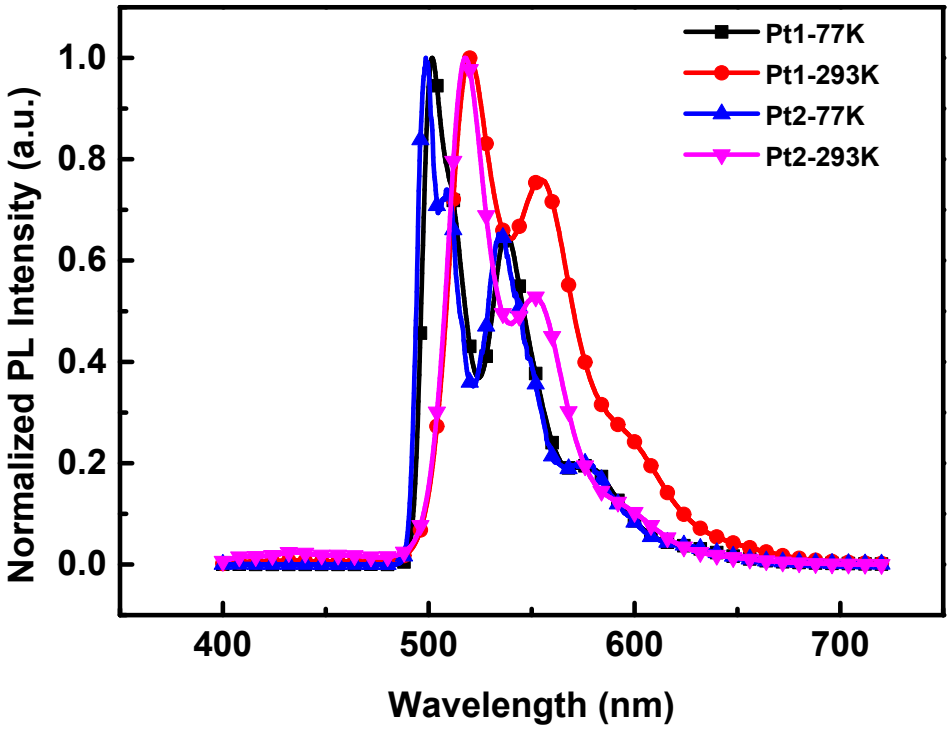

Figure S13. Photoluminescence spectra of **Pt1** and **Pt2** in degassed 2-methyltetrahydrofuran (2-MeTHF) at temperatures of T = 293 K and 77 K.

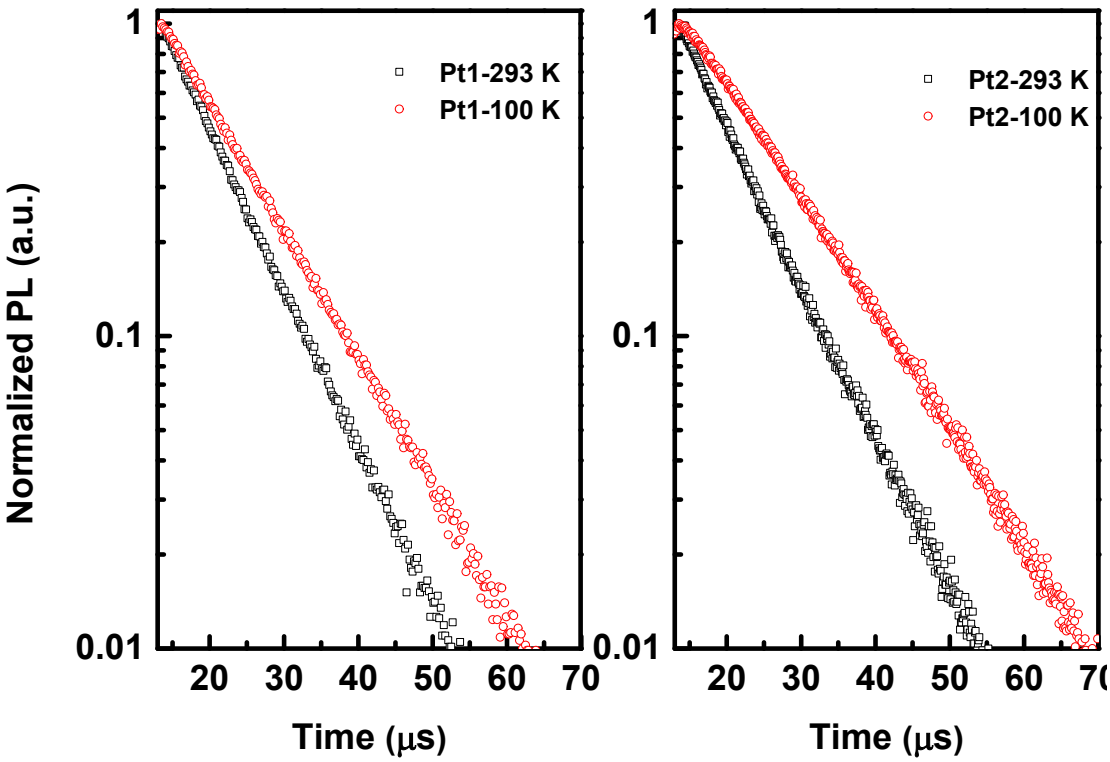

Figure S14. Transient phosphorescence decay of **Pt1** and **Pt2** in neat film obtained at T =293 and 100 K.

Table S2. The extracting triplet lifetimes (**τ**) at temperatures of T=100 K and 293 K

temperature	100 K	293 K
	τ (μs)	
Pt1	10.6	8.4
Pt2	11.6	9.3

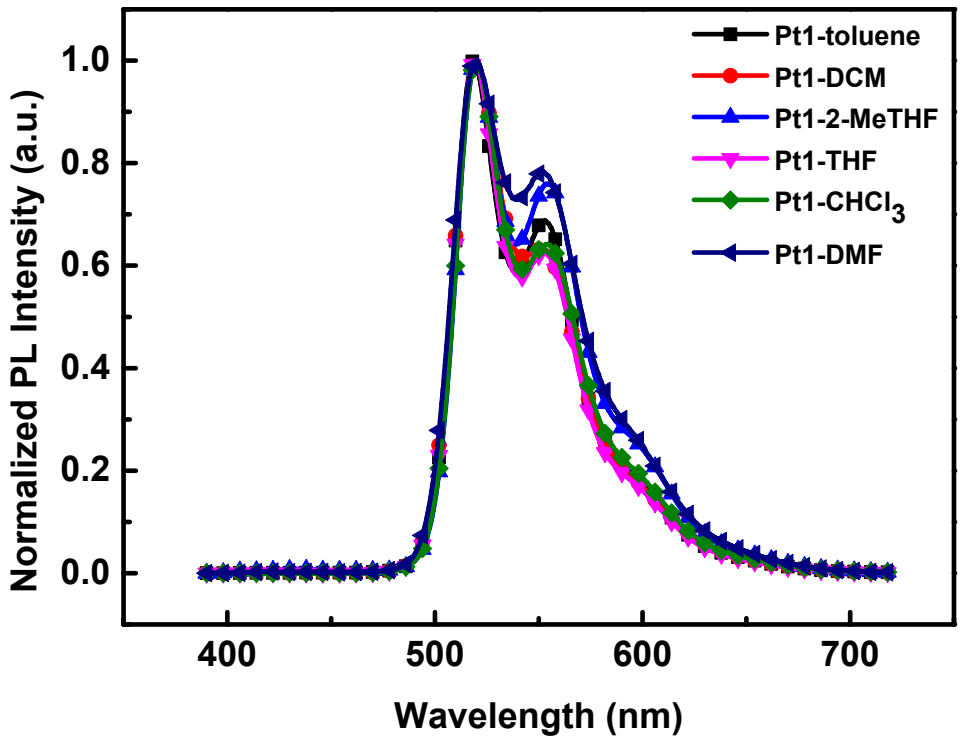

Figure S15. Photoluminescence spectra of diluted **Pt1** in different polarity media.

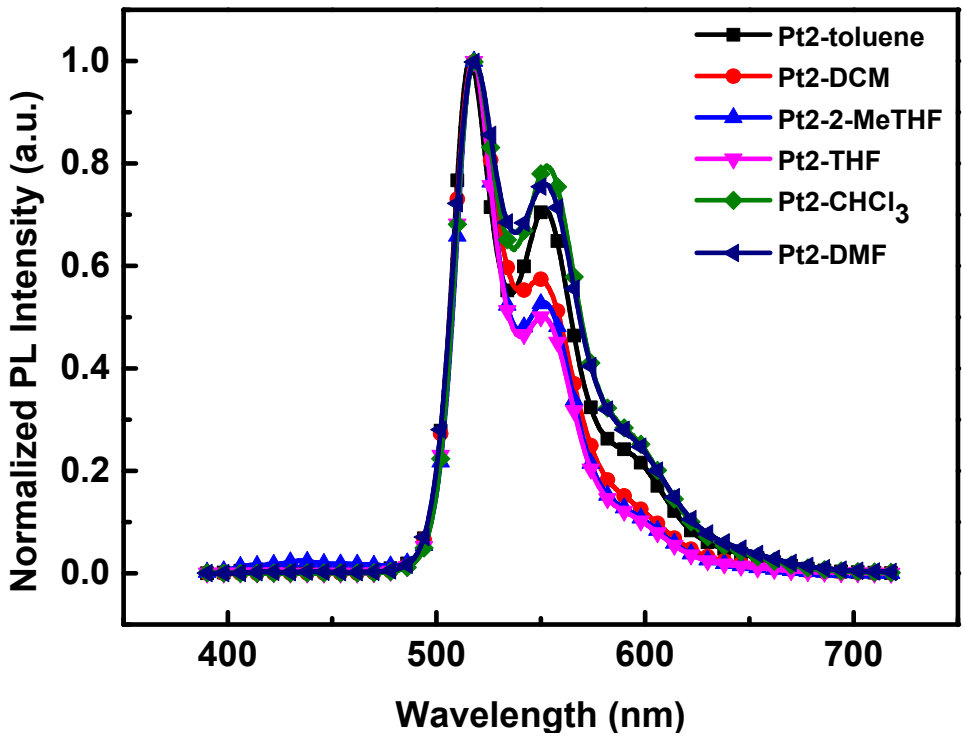

Figure S16. Photoluminescence spectra of diluted **Pt2** in different polarity media.

Table S3. DFT calculations of HOMO, LUMO, E_g, S_1 and T_1 for the platinum(II) complexes

	Pt1	**Pt2**
HOMO (eV)	-5.45	-5.29
LUMO (eV)	-1.79	-1.49
E_g (eV)	3.65	3.80
S_1 (eV)	2.90	3.00
T_1 (eV)	2.60	2.58

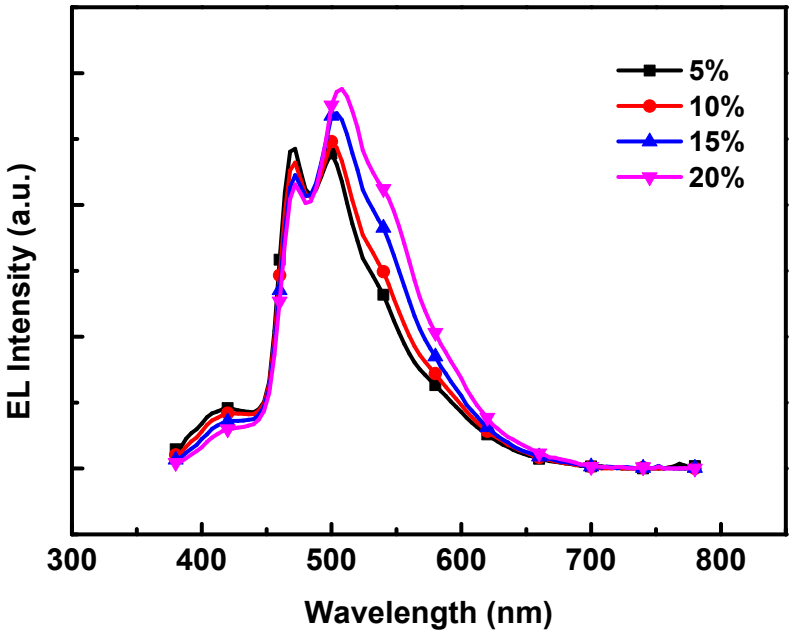

Figure S17. The EL spectra of complex **Pt1** in the mCP host with current density at 5 mA/cm^2.

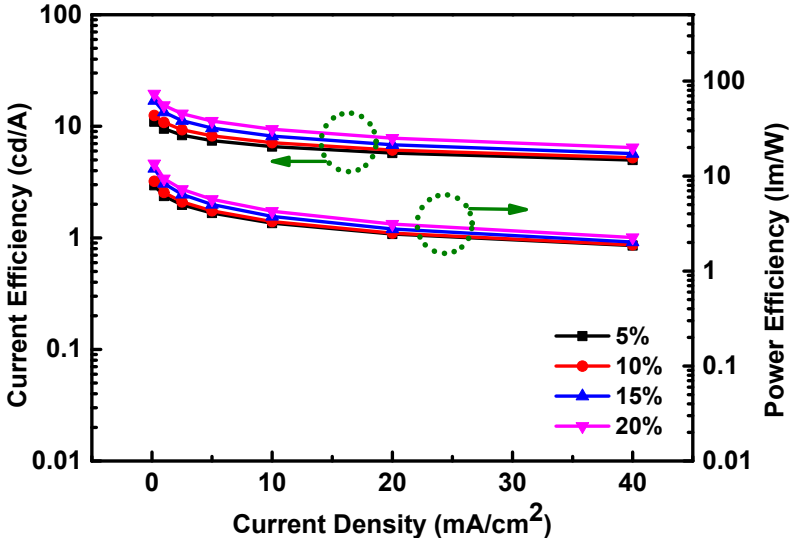

Figure S18. The power efficiency-current density-current efficiency curves for **Pt1** in the mCP host at different doping ratios.

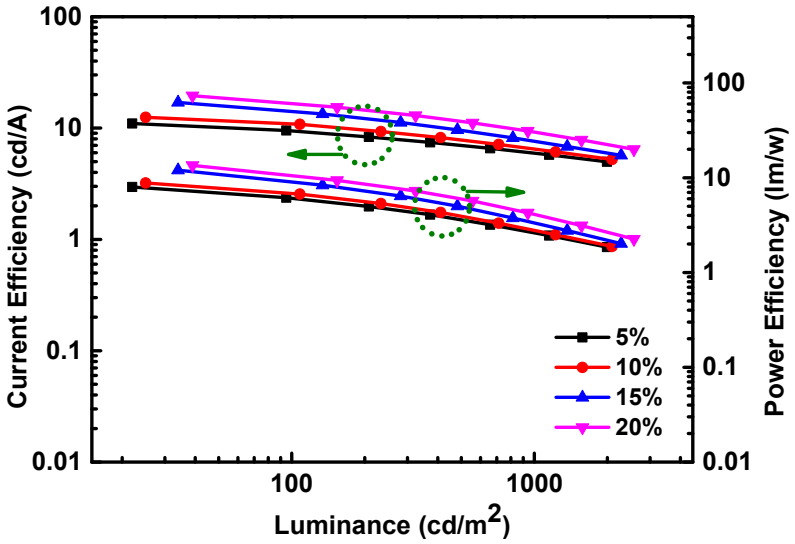

Figure S19. The power efficiency-luminance-current efficiency curves for **Pt1** in the mCP host at different doping ratios.

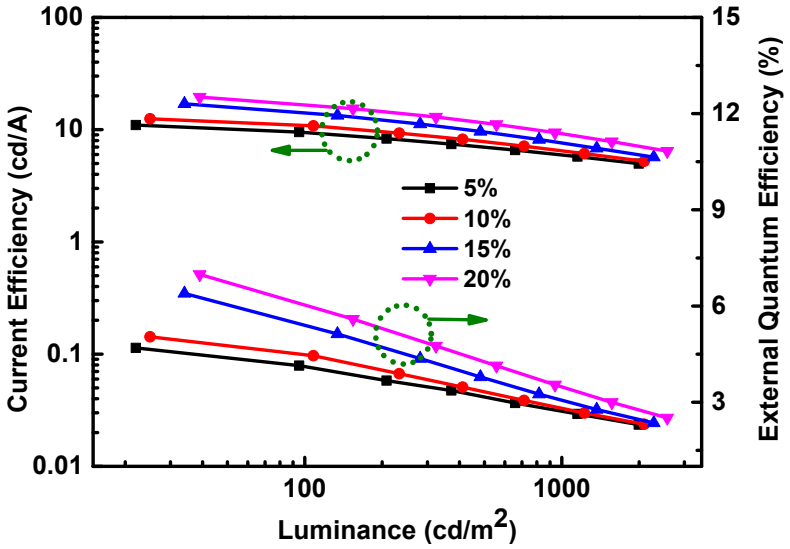

Figure S20. The EQE-luminance-current efficiency curves for **Pt1** in the mCP host at different doping ratios.

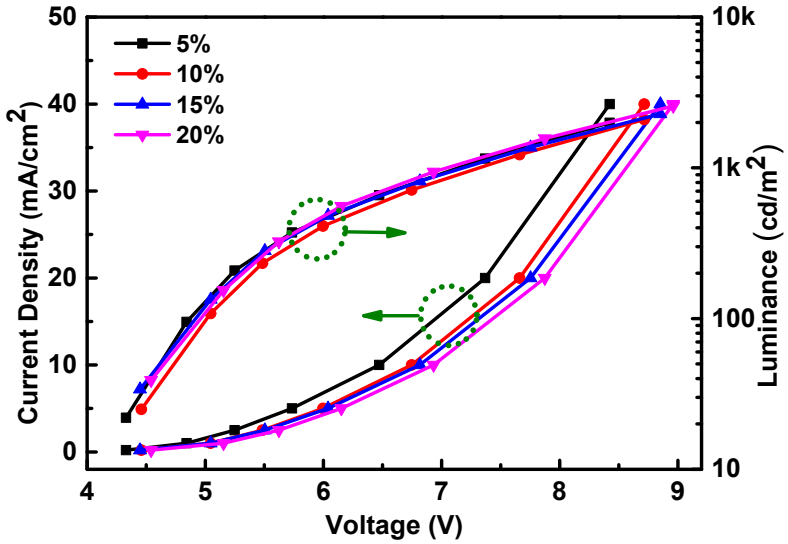

Figure S21. The current density-voltage-luminance curves for **Pt1** in the mCP host at different doping ratios.

Table S4. EL performance of the **Pt1** in the mCP host

Dopant	Dopant level [wt %]	$\eta_{c.max.}$/ $\eta_{c.500}$/$\eta_{c.1000}$ [cd A^{-1}] [a]			$\eta_{p.max.}$/ $\eta_{p.500}$/$\eta_{p.1000}$ [lm W^{-1}] [b]			$\eta_{EQE.max.}$/ η_{500}/η_{1000} [%] [c]			λ_{em} [nm]	λ_{sh} [nm]	CIE (x,y) [d]
Pt1	5	11.0	7.1	6.0	8.0	3.7	2.7	4.7	3.2	2.7	500	470	(0.21, 0.37)
	10	12.5	7.9	6.5	8.8	4.0	2.9	5.0	3.3	2.8	500	470	(0.22, 0.39)
	15	17.0	9.6	7.7	12.0	5.0	3.4	6.4	3.8	3.1	504	471	(0.23, 0.42)
	20	19.5	11.6	9.3	13.1	6.1	4.2	7.0	4.3	3.5	507	472	(0.25, 0.45)

[a)] Maximum current efficiency ($\eta_{c.max}$), and current efficiency ($\eta_{c.500}$, $\eta_{c.1000}$) measured at a brightness of 500 cd m^{-2} and 1000 cd m^{-2}, respectively; [b)] Maximum power efficiency ($\eta_{p.max}$), and power efficiency ($\eta_{p.500}$, $\eta_{p.1000}$) measured at a brightness of 500 cd m^{-2} and 1000 cd m^{-2}, respectively; [c)] Maximum external quantum efficiency ($\eta_{EQE.max.}$), and EQE ($\eta_{EQE.500}$, $\eta_{EQE.1000}$) measued at 500 cd m^{-2} and 1000 cd m^{-2}, respectively; [d)] Commission Internationale de L'Eclairage coordinates measured at 5 mA cm^{-2}.

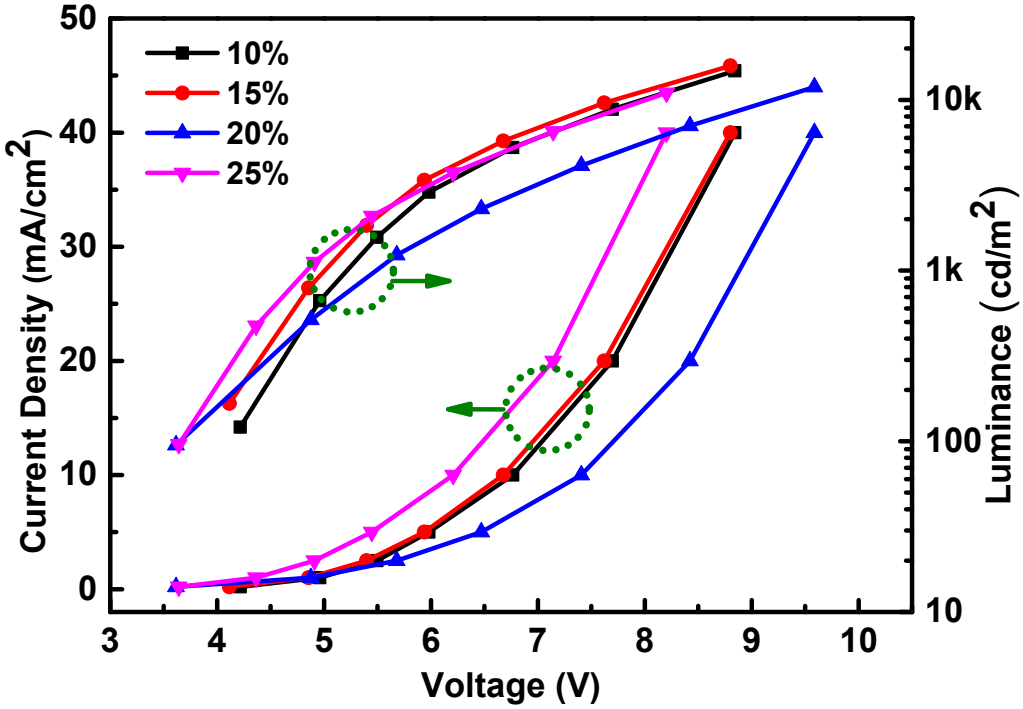

Figure S22. The current density-voltage-luminance curves for **Pt1** at different doping ratios.

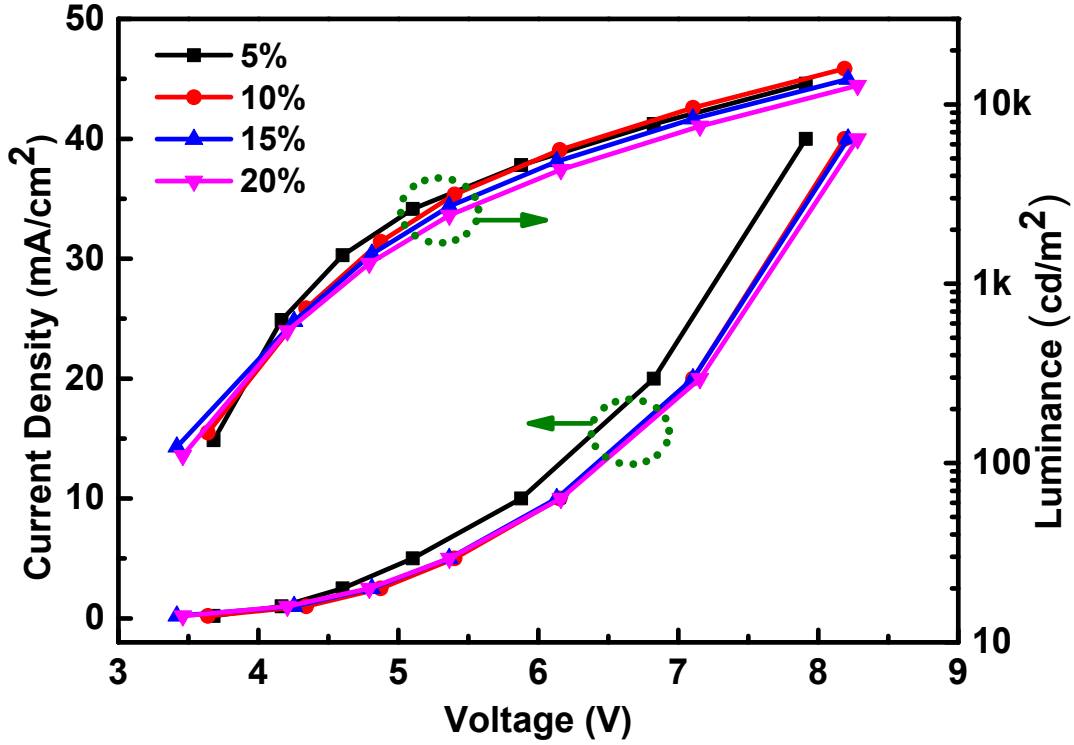

Figure S23. The current density-voltage-luminance curves for **Pt2** at different doping ratios.

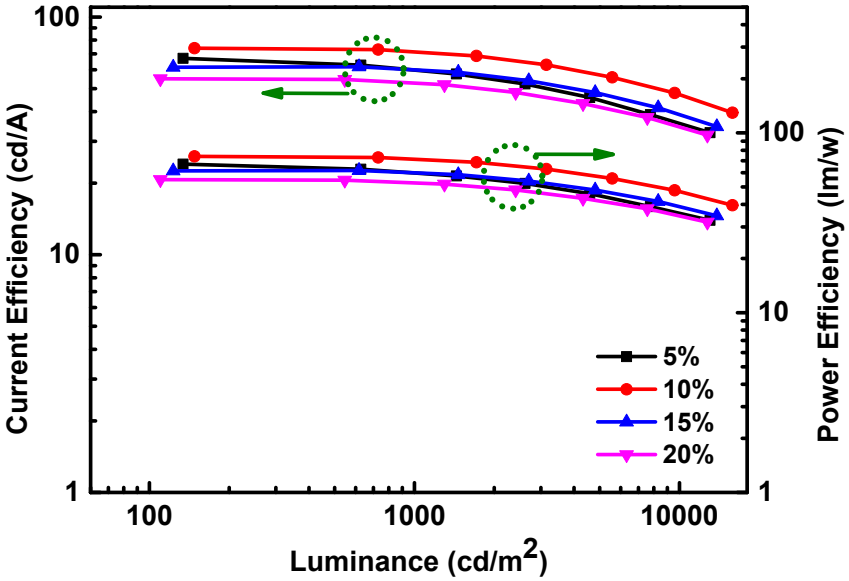

Figure S24. The power efficiency-luminance-current efficiency curves for **Pt2** at different doping ratios.

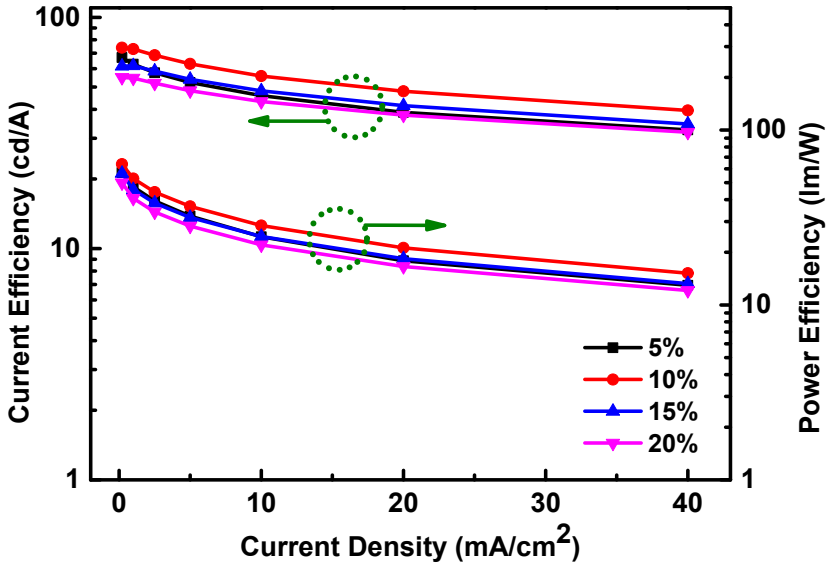

Figure S25. The power efficiency-current density-current efficiency curves for **Pt2** at different doping ratios.

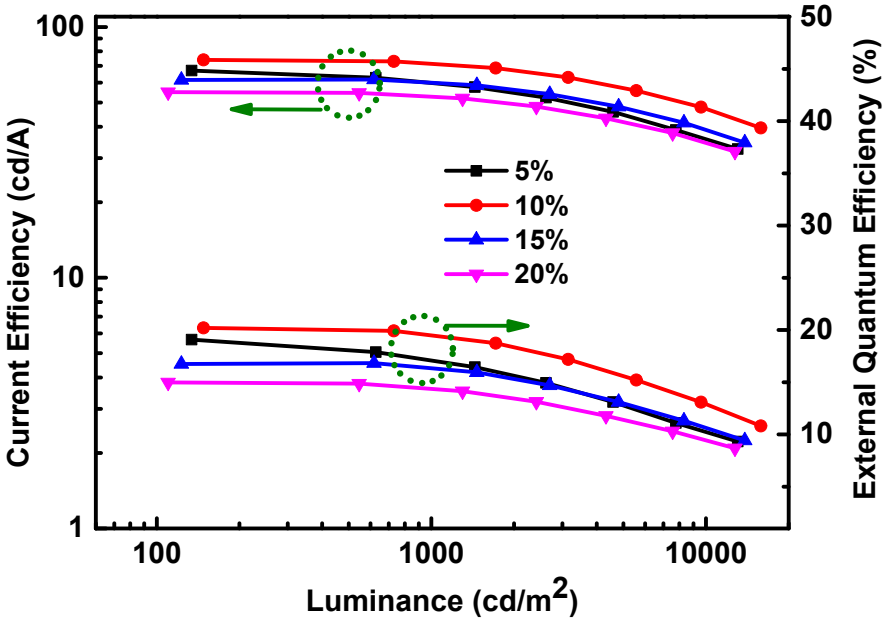

Figure S26. The EQE-luminance-current efficiency curves for **Pt2** at different doping ratios.

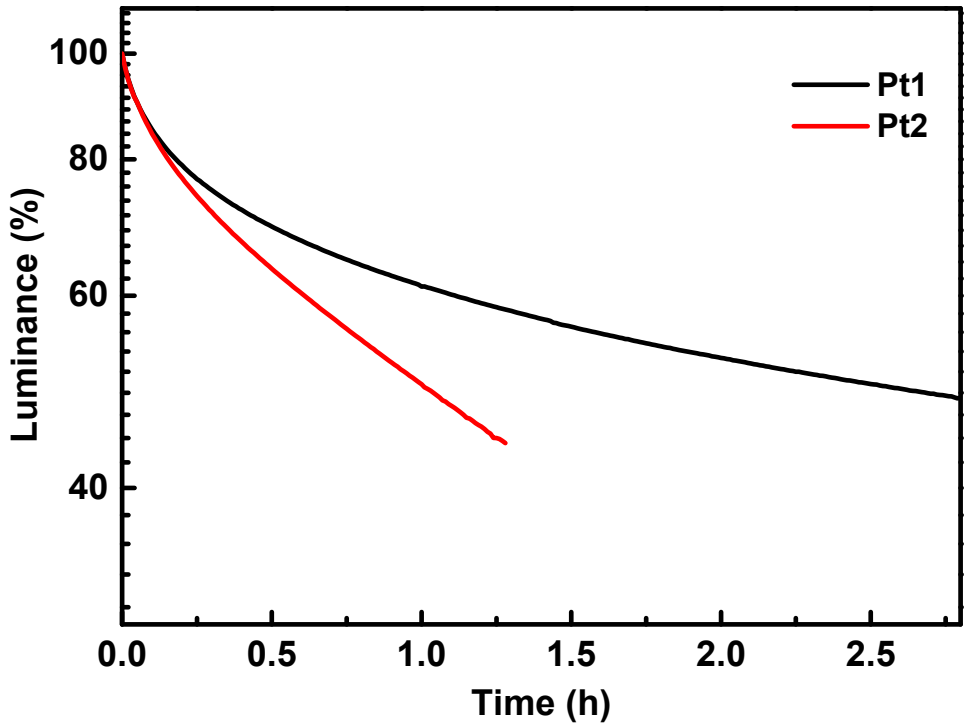

Figure S27. Lifetime curves of **Pt1** and **Pt2** devices at a luminance of 1000 cd/m^2.

Table S5. Crystal data and structure refinements for compounds **Pt1-Pt2**.

Compound	**Pt1**	**Pt2**
Empirical formula	$C_{42}H_{42}N_2O_2Pt$	$C_{41}H_{43}N_3O_2Pt$
Formula weight	801.87	804.87
Crystal system	Monoclinic	Monoclinic
Space group	$P2_1$	$P2_1/c$
a (Å)	10.0732(11)	14.3531(8)
b (Å)	31.516(3)	26.4522(15)
c (Å)	11.2075(12)	20.1764(12)
α (deg)	90.00	90.00
β (deg)	99.143(2)	106.8190(11)
γ (deg)	90.00	90.00
V (Å^3)	3512.8(6)	7332.7(7)
Z	4	8
D_c (g/cm^3)	1.516	1.458
μ (mm^{-1})	4.032	3.865
F (000)	1608	3232
Collcd reflns	18598	47538
Unique reflns	11424	17025
parameters	836	868
R_{int}	0.0530	0.0478
GOF	0.996	0.986
R_1[a] [I>2σ (I)]	0.0516	0.0411
wR_2[b] (all data)	0.1176	0.0917

[a]$R_1 = \sum||F_o|-|F_c||/\sum|F_o|$; [b]$wR_2 = \sum[w(F_o^2-F_c^2)^2]/\sum[w(F_o^2)^2]^{1/2}$.